JACS
JOURNAL OF THE AMERICAN CHEMICAL SOCIETY

Communication

pubs.acs.org/JACS

Induction of pH Sensitivity on the Fluorescence Lifetime of Quantum Dots by NIR Fluorescent Dyes

Rui Tang, Hyeran Lee, and Samuel Achilefu*

Department of Radiology, Washington University, St. Louis, Missouri 63110, United States

Supporting Information

ABSTRACT: Modulation of the fluorescence lifetime (FLT) of CdTeSe/ZnS quantum dots (QDs) by near-IR (NIR) organic chromophores represents a new strategy for generating reproducible pH-sensing nanomaterials. The hybrid construct transfers the pH sensitivity of photolabile NIR cyanine dyes to highly emissive and long-lifetime pH-insensitive QDs, thereby inducing a reproducible FLT change from 29 ns at pH >7 to 12 ns at pH <5. This approach provides an unparalleled large dynamic FLT range for pH sensing at NIR wavelengths.

Fluorescent molecular probes are useful for sensing many chemical and biological processes, such as pH, ligand binding, enzyme activity, and salt concentrations.[1−3] Because of the critical roles played by the acidity of the medium in biological systems,[4,5] a variety of intracellular pH reporting strategies with organic dyes have been developed.[6] Recent efforts to translate findings in cell assays to living organisms have led to concerted efforts to develop pH-sensitive near-IR (NIR) molecular probes and nanoparticles for assessing the functional status of both cells and tissue.[7−10] These sensors rely on fluorescence intensity measurements using a reference calibration model or ratiometric fluorescence techniques. The inherent difficulties with reproducibility of intensity measurements and the complexity of implementing quantitative in vivo measurements with emissions at disparate wavelengths (typically in the visible and NIR regions) have increased the interest in the use of the fluorescence lifetime (FLT) technique for pH sensing because the FLT is less dependent on several factors that perturb intensity measurements.[11−13]

Despite these advances, changes in the FLTs of NIR organic fluorophores in response to pH changes are marginal. Reported FLT changes between acidic and basic media are <1 ns. Another major limitation of using NIR organic dyes as pH sensors for intracellular pH measurements is their poor photostability, which is amplified in FLT techniques, where a longer signal integration time is typically needed. An alternative approach is to use semiconductor quantum dots (QDs), which offer significant advantages over conventional organic dyes. These include a broad absorption spectrum for flexibility in excitation wavelengths; large multiphoton action cross sections for efficient multiphoton microscopy; narrow, size-tunable emission for multicolor imaging; superior photostability for longitudinal studies; high quantum yield for improving detection sensitivity; and long fluorescence lifetime to minimize interference from naturally occurring organic fluorophores.[14−19] Although the intrinsic spectral insensitivity of QDs to environmental changes favors reproducibility of the fluorescence data, surface coatings or labeling have been shown to alter their spectral properties.[20] This feature has been used to develop biosensors where the QD fluorescence intensity is modulated by organic molecules through energy- or electron-transfer processes.[21−27] Most of these studies have been based on visible-light-emitting QDs and relied on spectral shifts or changes in luminescence intensity. Despite the enormous progress made with these hybrid nanomaterials, the need for NIR pH sensors with large dynamic measurement parameters for in vitro, cellular, and in vivo applications remains unmet.

Our goal in this study was to develop a general strategy for generating photostable NIR pH sensors with large dynamic pH-sensing capability. The hybrid constructs incorporate the excellent photophysical properties of QDs with the high pH sensitivity of NIR organic dyes. Inversion of the pH response can be achieved by switching from Förster resonance energy transfer (FRET) to photoinduced electron transfer (PET) quenching processes.

We first prepared the pH-sensitive NIR carbocyanine dye LS662 (Scheme 1) by the method described previously.[7] LS662

Scheme 1. Illustration of the Processes Involved in QD pH Sensing Induced by pH-Sensitive Organic Dyes

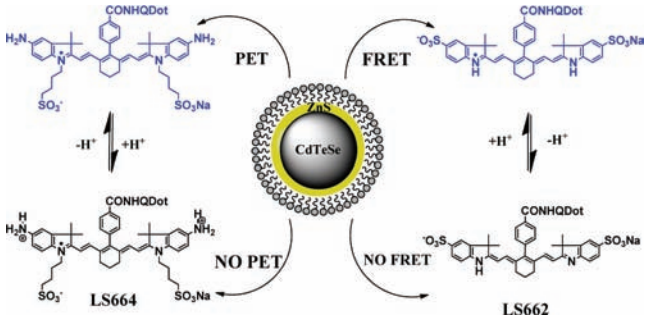

exhibits an absorption maximum in the NIR (750 nm) at low pH that undergoes a hypsochromic shift to the visible region (520 nm) with increasing pH, with a pK_a of 5.2 [Figure S1 in the Supporting Information (SI)]. Above pH 7, the dye fluorescence is insignificant. The dye itself is not suitable for FLT pH measurements because of its <0.2 ns FLT change in the physiologically useful pH range of 4−7. However, these

Received: January 10, 2012
Published: February 23, 2012

dx.doi.org/10.1021/ja300276s | J. Am. Chem. Soc. 2012, 134, 4545−4548

spectral properties are suitable for the development of FRET-based QD pH sensors through modulation of the emission properties of the QDs at either 520 or 750 nm with LS662.

CdTeSe QDs coated with ZnS and capped with cysteamine were synthesized and then conjugated to LS662 (Scheme 1). The hybrid nanomaterials were purified by either dialysis or centrifugation followed by removal of the supernatant (see the SI for detailed synthesis procedures and characterization of CdTeSe/ZnS QDs and the QD−organic dye conjugates). The cysteamine ligands served as amine-reactive functionality and aided the stabilization and solubility of the colloidal QDs in aqueous media across a wide pH range.

Transmission electron microscopy (TEM) of the QD−dye conjugates showed an average diameter of 9.4 nm with a fairly monodisperse distribution (Figure 1A,B). Both the organic

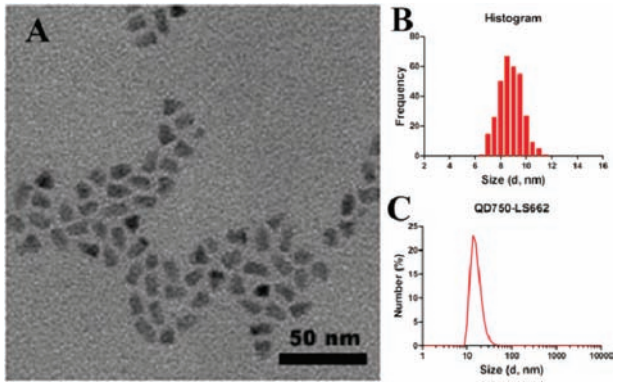

Figure 1. (A) Representative TEM image of the QD750−LS662 construct. The scale bar is 50 nm. (B) Histogram of the particle sizes measured from TEM images, giving an average diameter of 9.37 ± 1.13 nm (±12.1%). (C) DLS data for QD750−LS662, showing a hydrodynamic diameter of 18.17 ± 2.40 nm (±13.2%).

surface ligands and the conjugated dye molecules increased the QD hydrodynamic diameter to ~18.2 nm (Figure 1C), as determined by dynamic light scattering (DLS). From deconvolution of the absorption spectrum of the QD−dye conjugates, a QD/dye ratio of 1:8 was calculated (Figure S4).

For accurate reporting of the dye-modulated pH response, the QDs and surface coatings should lack inherent pH sensitivity and have luminescence near 520 or 750 nm to match the spectral shift of LS662. Spectral analysis showed that the luminescence intensity of the parent cysteamine-coated CdTeSe/ZnS QDs with 750 nm luminescence (QD750) lacked pH sensitivity (Figure S2). In contrast, the QD750−dye conjugates displayed a biphasic absorption response to pH (Figure 2A). Unlike LS662, which exhibited an inverse relationship with increasing pH at 770 nm, the 750 nm luminescence of QD750 in the QD750−LS662 conjugates increased with increasing pH (Figure 2B).

Because the FRET efficiency is determined by the extent of spectral overlap between the QD emission and the dye absorption, pH-dependent spectral shifts of the dye absorption alter the FRET efficiency. On the basis of the spectral properties of LS662, QD750 luminescence has excellent spectral overlap with the dye's NIR absorption at low pH. This allows energy transfer from the QDs to the dye molecules, resulting in the quenching of the QD emission. Additional quenching could be induced by PET from the dye's tertiary amine to the QD.[28] The expected shift in the dye's absorption

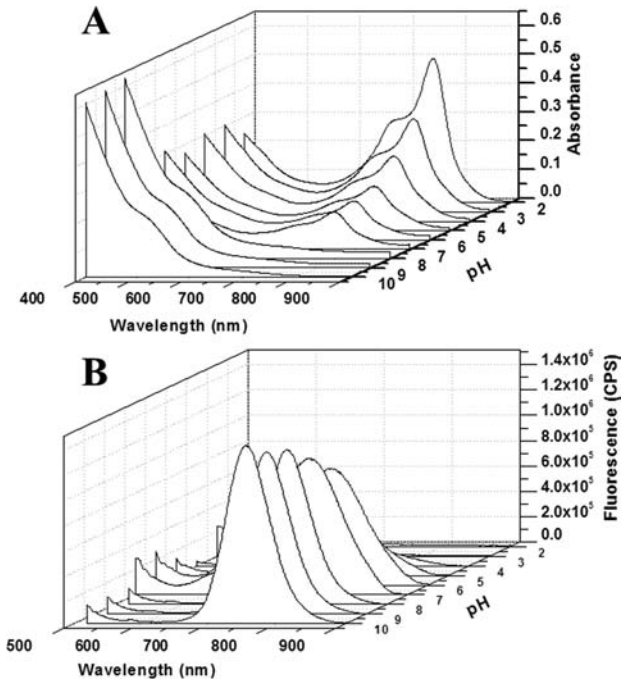

Figure 2. (A) UV−vis absorption spectra of QD750−LS662 conjugates at different pH values. (B) Fluorescence spectra of the QD750−LS662 conjugates at different pH values. The excitation wavelength was 488 nm.

from 750 to 520 nm at basic pH produced high QD750 luminescence (Figure 2). The small Stokes shift of the NIR dye, coupled with the significant overlap of its fluorescence with the QD750 emission, complicated the determination of the FRET efficiency using changes in fluorescence intensity. However, this parameter could be determined using FLT measurements.

Toward this goal, we explored the FLT-based pH sensitivity of the QD750−dye conjugates in different buffer solutions. The FLT of the QDs alone has a small pH response, varying between 29 and 31 ns (Figure S2C). This narrow FLT change represents <10% of the native QD FLT and does not have the dynamic FLT range needed for pH sensing in heterogeneous media. In contrast, the FLT decay profile of the 750 nm emission of the QD750−dye conjugates showed a significant pH response (Figure 3A), decreasing from 29 ns at pH >7 to

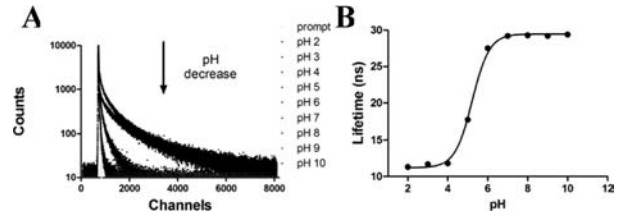

Figure 3. (A) FLT decay profile of the QD750−LS662 conjugates at different pH values. (B) Sigmoidal fit of the FLT vs pH curve, giving a pK_a of 5.2.

12 ns at pH <5. A plot of the FLT versus pH showed a sigmoidal transition with a pK_a of 5.2 (Figure 3B). This plot mirrored that of the dye using fluorescence intensity measurements (Figure S1), exhibiting the same pK_a but a reversal of the intensity versus pH response. This demonstrates that the organic dye imparted its pH sensitivity to the QDs with high accuracy, providing a general strategy for improving the

dx.doi.org/10.1021/ja300276s | J. Am. Chem. Soc. 2012, 134, 4545−4548

photostability and signal dynamic range of pH-sensitive organic molecules.

To determine the FRET efficiency (E) by FLT, we used the equation $E = 1 - \tau_a/\tau_b$, where τ_a is 12 ns (the QD750 FLT at pH 2, where all of the dye absorption overlaps with the QD750 emission) and τ_b is 29 ns (determined at pH 10, where no dye absorption overlaps with the QD750 emission). This gave $E \approx$ 60%, validating the choice of the FLT instead of the emission intensity as the pH-reporting parameter. At 60%, however, residual QD emission is still significant, and without a ratiometric strategy, quantitative pH measurement in cells and tissue would otherwise be complicated.

A potential strategy for incorporating ratiometric pH sensing would be to label with LS662 two different QDs emitting at 520 and 750 nm to match the absorption shift of the dye at different pH. Thus, we prepared QD560–LS662 conjugates, which were designed to have spectral overlap with the LS662 absorption in neutral to basic pH media (Figure S5A). As expected, FRET efficiency of this construct increased with increasing pH, resulting in a reversed FLT trend relative to that for QD750–LS662 (Figure S5B,C). The 560 nm emission of the QD560–LS662 conjugates also showed a significant FLT change from 7 ns at pH >7 to 31 ns at pH <5, with pK_a = 5.5 and $E \approx$ 77% between pH 2 (31 ns) and pH 10 (7 ns). Thus, FLT alone or a ratiometric pH measurement with the combination of QD560–LS662 and QD750–LS662 can successfully be used to determine the pH of chemical and biological systems quantitatively.

To validate that the induction of the pH sensitivity on the QDs originated from the pH-sensitive organic dye, we conjugated QD750 to a non-pH-sensitive dye, LS288 (Figure S8). This dye has absorption and emission maxima at 760 and 780 nm, respectively. The photophysical properties of this dye, including the absorption, emission, and FLT of QD750–LS288 construct, were investigated at different pH values (Figure S6). Upon conjugation of the dye to QD750, a significant pH-independent emission quenching occurred, resulting in an E value of ~73% at all pH values between 2 and 10, where E was determined by defining τ_a and τ_b as the FLTs after (7 ns) and before (26 ns) dye conjugation. This finding could be used to develop stable, activatable probes that will restore the QD fluorescence after removal of the non-pH sensitive-dye by enzymes or other biological events. More importantly, the result confirms the role of the organic pH-sensitive dye in imparting pH sensitivity to the QDs.

To explore the generality of the pH-sensing strategy, we prepared the pH-sensitive heptamethine dye LS664, which exhibits fluorescence in an acidic environment that is quenched by a PET mechanism under neutral and basic conditions (Scheme 1 and Figure S7). This dye has an absorption maximum at 760 nm below pH 4 that shifts to 810 nm above pH 5, generating the nonfluorescent analogue. Both absorption and emission spectral analyses at different pH values gave a pK_a of 3.2. Using a method similar to the one described for the synthesis of QD750, we prepared cysteamine-coated CdTeSe/ZnS QDs emitting at 760 nm (QD760, Figure S9) to overlap with the absorption maximum of LS664 under acidic conditions. The QD760–LS664 conjugates were prepared, and their pH-dependent FLT response was investigated (Figure 4). If FRET were the primary quenching mechanism, we would expect QD emission quenching at pH <4 and significant emission intensity at pH >5. Instead, the QD emission quenching increased with pH, as reflected by the FLT plot

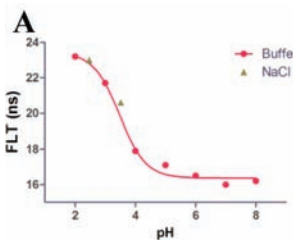

pH	Buffer	NaCl solution
2.00	23.2	
2.47		23.0
3.00	21.7	
3.52		20.6
4.00	17.9	
5.00	17.1	
6.00	16.5	
7.00	16.0	
8.00	16.2	

Figure 4. (A) FLT profile of the QD760–LS664 conjugates. The red solid line is a sigmoidal fit of the data, which gave a pK_a of 3.5. (B) Table of lifetimes obtained from QD760–LS664 conjugates at different pH; hydrion buffers were used. Two additional points were added between pH 2 and 4 by titrating a 0.1 M NaCl solution using HCl or NaOH to optimize the sigmoidal fit of the titration curve.

(Figure 4). The mechanism of luminescence quenching and enhancement by LS664 is not fully understood at this time, but previous studies have shown that amines are electron donors to QDs and could be involved in PET-mediated QD emission quenching.[28] Although QD760 was coated with cysteamine, which could serve as an electron donor under basic conditions, we did not observe PET with the analogous QD750 QDs. Since the major difference between the two QD formulations are the dyes, we attribute this quenching to PET from the amine groups on the indolium ring of LS664 to the QDs under basic conditions. The pK_a value obtained from the sigmoidal fit of the lifetime decay profile was 3.5, which is also consistent with the pK_a of LS664 alone. This demonstrates the feasibility of applying pH-sensitive dyes with PET capability to modulate the FLT of QDs. However, delineation of the exact process by which LS664 perturbs the spectral properties of the QDs needs further exploration.

In summary, we have developed new pH-sensitive QD–organic dye hybrid nanomaterials in which the pH-sensing properties of NIR dyes are imparted to photostable QDs, resulting in large FLT sensitivity scale. In particular, perturbation of the FLT of the QDs by FRET or PET processes illustrates the generality of the approach. The QD FRET donors can be readily custom-engineered to match the absorption features of the pH-sensitive dye acceptor used to modulate the FLT of QDs. This new approach allows environmentally insensitive QDs to become highly efficient pH sensors for a variety of potential environmental and biological applications. For example, the large two-photon (2P) action cross sections of QDs and the deep tissue penetration of NIR light ideally position these sensors for use in multiphoton microscopy of molecular processes across large spatial scales ranging from cells to thick tissue. Moreover, direct 2P excitation of the highly photostable QDs prevents the rapid photobleaching of the pH-sensitive cyanine NIR dyes, which readily occurs under irradiation with high-intensity lasers.

■ ASSOCIATED CONTENT

Supporting Information

Detailed experimental methods, dye structures, spectral properties of different constructs, deconvolution of the spectra, and pK_a measurements. This material is available free of charge via the Internet at http://pubs.acs.org.

■ AUTHOR INFORMATION

Corresponding Author

achilefus@mir.wustl.edu

Notes

The authors declare no competing financial interest.

■ ACKNOWLEDGMENTS

This study was based upon work supported by the NIH Grants R01 EB007276 and R01 EB008111; and in part by R33 CA123537, U54 CA136398 (Network for Translational Research), and HHSN268201000046C (NHLBI Program of Excellence in Nano-technology).

■ REFERENCES

(1) Dahan, M.; Levi, S.; Luccardini, C.; Rostaing, P.; Riveau, B.; Triller, A. *Science* **2003**, *302*, 442.
(2) Michalet, X.; Pinaud, F. F.; Bentolila, L. A.; Tsay, J. M.; Doose, S.; Li, J. J.; Sundaresan, G.; Wu, A. M.; Gambhir, S. S.; Weiss, S. *Science* **2005**, *307*, 538.
(3) Lidke, D. S.; Nagy, P.; Heintzmann, R.; Arndt-Jovin, D. J.; Post, J. N.; Grecco, H. E.; Jares-Erijman, E. A.; Jovin, T. M. *Nat. Biotechnol.* **2004**, *22*, 198.
(4) Casey, J. R.; Grinstein, S.; Orlowski, J. *Nat. Rev. Mol. Cell Biol.* **2010**, *11*, 50.
(5) Srivastava, J.; Barber, D. L.; Jacobson, M. P. *Physiology (Bethesda)* **2007**, *22*, 30.
(6) Han, J.; Burgess, K. *Chem. Rev.* **2010**, *110*, 2709.
(7) Lee, H.; Akers, W.; Bhushan, K.; Bloch, S.; Sudlow, G.; Tang, R.; Achilefu, S. *Bioconjugate Chem.* **2011**, *22*, 777.
(8) Hilderbrand, S. A.; Kelly, K. A.; Niedre, M.; Weissleder, R. *Bioconjugate Chem.* **2008**, *19*, 1635.
(9) Patonay, G.; Casay, G. A.; Lipowska, M.; Strekowski, L. *Talanta* **1993**, *40*, 935.
(10) Chen, Y.; Li, X. *Biomacromolecules* **2011**, *12*, 4367.
(11) Povrozin, Y. A.; Markova, L. I.; Tatarets, A. L.; Sidorov, V. I.; Terpetschnig, E. A.; Patsenker, L. D. *Anal. Biochem.* **2009**, *390*, 136.
(12) Berezin, M. Y.; Guo, K.; Akers, W.; Northdurft, R. E.; Culver, J. P.; Teng, B.; Vasalatiy, O.; Barbacow, K.; Gandjbakhche, A.; Griffiths, G. L.; Achilefu, S. *Biophys. J.* **2011**, *100*, 2063.
(13) Almutairi, A.; Guillaudeu, S. J.; Berezin, M. Y.; Achilefu, S.; Fréchet, J. M. J. *J. Am. Chem. Soc.* **2008**, *130*, 444.
(14) Murray, C. B.; Norris, D. J.; Bawendi, M. G. *J. Am. Chem. Soc.* **1993**, *115*, 8706.
(15) Parak, W. J.; Gerion, D.; Pellegrino, T.; Zanchet, D.; Micheel, C.; Williams, S. C.; Boudreau, R.; Le Gros, M. A.; Larabell, C. A.; Alivisatos, A. P. *Nanotechnology* **2003**, *14*, R15.
(16) Clapp, A. R.; Medintz, I. L.; Mauro, J. M.; Fisher, B. R.; Bawendi, M. G.; Mattoussi, H. *J. Am. Chem. Soc.* **2004**, *126*, 301.
(17) Medintz, I. L.; Konnert, J. H.; Clapp, A. R.; Stanish, I.; Twigg, M. E.; Mattoussi, H.; Mauro, J. M.; Deschamps, J. R. *Proc. Natl. Acad. Sci. U.S.A.* **2004**, *101*, 9612.
(18) Murphy, C. J. *Anal. Chem.* **2002**, *74*, 520A.
(19) Dabbousi, B. O.; Rodriguez-Viejo, J.; Mikulec, F. V.; Heine, J. R.; Mattoussi, H.; Ober, R.; Jensen, K. F.; Bawendi, M. G. *J. Phys. Chem. B* **1997**, *101*, 9463.
(20) Medintz, I. L.; Stewart, M. H.; Trammell, S. A.; Susumu, K.; Delehanty, J. B.; Mei, B. C.; Melinger, J. S.; Blanco-Canosa, J. B.; Dawson, P. E.; Mattoussi, H. *Nat. Mater.* **2010**, *9*, 676.
(21) Tomasulo, M.; Yildiz, I.; Raymo, F. M. *J. Phys. Chem. B* **2006**, *110*, 3853.
(22) Snee, P. T.; Somers, R. C.; Nair, G.; Zimmer, J. P.; Bawendi, M. G.; Nocera, D. G. *J. Am. Chem. Soc.* **2006**, *128*, 13320.
(23) Mattoussi, H.; Mauro, J. M.; Goldman, E. R.; Anderson, G. P.; Sundar, V. C.; Mikulec, F. V.; Bawendi, M. G. *J. Am. Chem. Soc.* **2000**, *122*, 12142.
(24) Bruchez, M.; Moronne, M.; Gin, P.; Weiss, S.; Alivisatos, A. P. *Science* **1998**, *281*, 2013.
(25) Chan, W. C.; Nie, S. *Science* **1998**, *281*, 2016.
(26) Goldman, E. R.; Anderson, G. P.; Tran, P. T.; Mattoussi, H.; Charles, P. T.; Mauro, J. M. *Anal. Chem.* **2002**, *74*, 841.
(27) Goldman, E. R.; Medintz, I. L.; Whitley, J. L.; Hayhurst, A.; Clapp, A. R.; Uyeda, H. T.; Deschamps, J. R.; Lassman, M. E.; Mattoussi, H. *J. Am. Chem. Soc.* **2005**, *127*, 6744.
(28) Tomasulo, M.; Yildiz, I.; Kaanumalle, S. L.; Raymo, F. M. *Langmuir* **2006**, *22*, 10284.